This article has been accepted for publication in a future issue of this journal, but has not been fully edited. Content may change prior to final publication. Citation information: DOI 10.1109/TCSII.2018.2803076, IEEE Transactions on Circuits and Systems II: Express Briefs

Design of a Broadband Wilkinson Power Divider with Wide Range Tunable Bandwidths by Adding a Pair of Capacitors

Anqi Chen, Yuan Zhuang, *Student Member, IEEE*, Jiafeng Zhou, Yi Huang, *Senior Member, IEEE*, and Lei Xing

***Abstract*—In this brief, a novel two-way power divider with a wide range tunable bandwidth is presented and investigated. The proposed power divider is designed based on adding a pair of capacitors in parallel with the transmission lines in a Trantanella-type of Wilkinson power divider. The proposed power divider provides an additional zero-reflection frequency which will significantly increase the bandwidth compared with a conventional Wilkinson power divider. Moreover, the added zero-reflection frequency is sensitive to the capacitors so that the bandwidth can be tuned by altering the capacitance of the capacitors. Analytic design methods and formulas are derived and presented in detail. A two-way power divider is designed and measured to validate the proposed method. The measurement indicates that the device has a 15-dB bandwidth of f_H/f_L=2.73:1 (0.75 GHz to 2.05 GHz). The proposed method can be applied for multi-way multi-section power dividers. Meanwhile, an eight-way power divider is designed and fabricated. The measured response has a bandwidth of f_H/f_L=2.67:1 (0.75 GHz to 2 GHz) with all the S-parameters better than -13 dB. The proposed power dividers have a wide bandwidth, compact size, good physical and electrical isolation feature. The measurement agrees well with the theoretical prediction which validates the proposed design theory.**

***Index Terms*—Broadband, isolation circuits, paralleled capacitors, power dividers, tunable bandwidth.**

I. Introduction

POWER dividers are essential components for many microwave applications in communication systems, such as antenna arrays and power amplifiers. The features of power dividers in terms of bandwidth, circuit size, insertion loss and isolation will significantly influence the overall performance of the communication system. A Wilkinson-type power divider [1] is one of the most widely used dividers due to its simple structure and low insertion loss. However, the isolation circuit that is connected to two output ports only provides electrical isolation but not physical separation to the circuit. In 2010, Trantanella [2] presented a novel power divider by placing the isolation elements between the λ/4 transmission lines at an arbitrary phase angle instead of 90° as in a conventional Wilkinson divider to enhance both electrical isolation and physical separation simultaneously. The structure has been investigated in depth in [3].

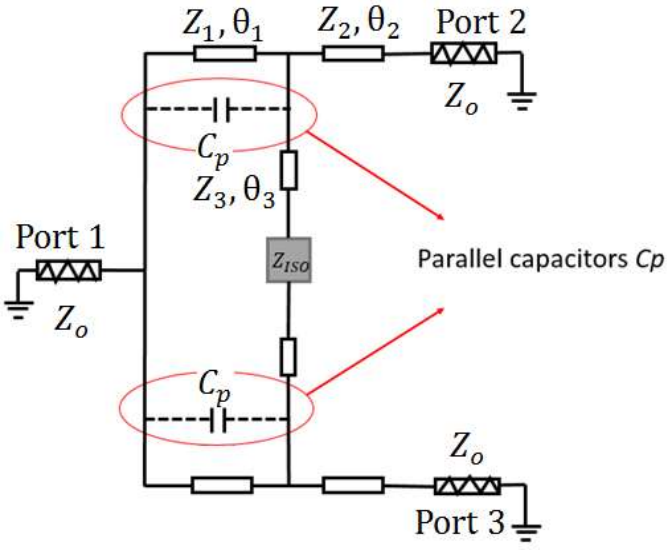

Fig. 1. The proposed broadband bandwidth tunable power divider.

Nowadays, frequency-tunable devices are attracting more and more attentions because they can integrate diverse operating frequency bands in a single device [4] [5]. A reconfigurable power divider based on the Trantanella structure was presented in [6] where the center frequency can be changed from 0.85 GHz to 2.4 GHz by tuning the bias voltage on the varactor diodes. However, the effective bandwidth for each operational band is narrow. A novel broadband power divider with wide range tunable bandwidths is presented in this brief. The idea is to add a pair of capacitors in parallel with the transmission lines as shown in Fig. 1.The proposed structure introduces an additional zero-reflection frequency to broaden the operational bandwidth and make the bandwidth tunable.

A. Chen, Y. Zhuang, J. Zhou and Y. Huang are with the Department of Electrical Engineering and Electronics, University of Liverpool, Liverpool, UK (email: Zhouj@liverpool.ac.uk).

L. Xing is with the College of Electronic and Information Engineering, Nanjing University of Aeronautics and Astronautics, Nanjing, China (email: xinglei@nuaa.edu.cn).

This article has been accepted for publication in a future issue of this journal, but has not been fully edited. Content may change prior to final publication. Citation information: DOI 10.1109/TCSII.2018.2803076, IEEE Transactions on Circuits and Systems II: Express Briefs

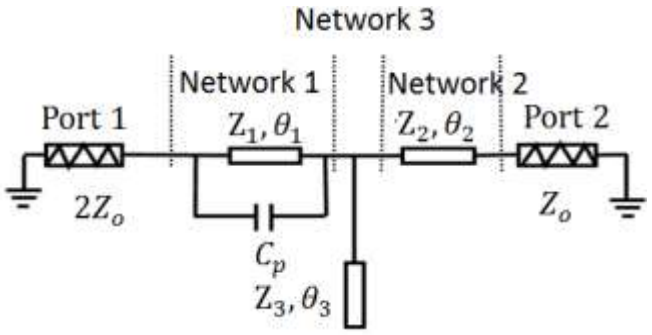

Fig. 2. Even-mode equivalent circuit for the proposed divider.

The idea of inserting a parallel capacitor has been reported in [7] to improve the out-of-band selectivity. The relationship between the variations of capacitance and the return loss has not yet been analytically discussed. This brief provides mathematic proof and design guidance on controlling the added zero-reflection frequency for tunable bandwidths. The structure and design theory are discussed in Section II. The relationships between the electrical length of transmission lines, zero-reflection frequency, and capacitance of added capacitors are illustrated and analyzed in Section III. In Section IV, a two-way and an eight-way three-section power divider are designed, fabricated and measured to validate the proposed design method. Conclusions are drawn finally in Section V.

II. DESIGN

A conventional Wilkinson power divider is perfectly matched at all ports at the center frequency, so that there is only one reflection zero in the passband. To broaden the bandwidth, an additional reflection zero at f_z can be generated by adding a pair of capacitors. As shown in Fig. 1, C_P denotes the added capacitors. Z_0 stands for the port impedance which is 50 Ω here. θ_1, θ_2, and θ_3 represent the electrical lengths of the transmission lines at 1 GHz. Z_1, Z_2, and Z_3 are the characteristic impedances of the transmission lines. Z_{ISO} represents the complex impedance isolation component. There will be two minimum-reflection frequencies for the proposed divider, one is near the original zero-reflection frequency $f_o = 1$ GHz and the other is the additional zero-reflection frequency f_z. By carefully choosing the values of the capacitors, the additional zero-reflection frequency f_z can significantly extend the operational bandwidth of the device. Details will be discussed in the following subsections.

A. Return Loss

The equivalent circuit of the proposed power divider under even-mode excitation is shown in Fig. 2. The circuit can be divided into three sub-networks. The ABCD matrix of the circuit is derived as:

$$\begin{vmatrix} \overline{A} & \overline{B} \\ \overline{C} & \overline{D} \end{vmatrix} = \begin{vmatrix} \overline{Y} - \frac{1}{\sqrt{2}\tan(\theta_1 \overline{f})} & \frac{1}{j(\overline{Y} - \frac{1}{\sqrt{2}\sin(\theta_1 \overline{f})})} \\ \overline{Y} - \frac{1}{\sqrt{2}\sin(\theta_1 \overline{f})} & \overline{Y} - \frac{1}{\sqrt{2}\tan(\theta_1 \overline{f})} \\ \hline (\overline{Y} - \frac{1}{\sqrt{2}\sin(\theta_1 \overline{f})})^2 - (\overline{Y} - \frac{1}{\sqrt{2}\tan(\theta_1 \overline{f})})^2 & \overline{Y} - \frac{1}{\sqrt{2}\sin(\theta_1 \overline{f})} \\ j(\overline{Y} - \frac{1}{\sqrt{2}\sin(\theta_1 \overline{f})}) & \end{vmatrix} \bullet \begin{vmatrix} 1 & 0 \\ j\frac{\tan(\theta_3 \overline{f})}{\sqrt{2}} & 1 \end{vmatrix} \bullet \begin{vmatrix} \cos(\theta_2 \overline{f}) & j\sqrt{2}\sin(\theta_2 \overline{f}) \\ j\frac{\sin(\theta_2 \overline{f})}{\sqrt{2}} & \cos(\theta_2 \overline{f}) \end{vmatrix} \quad (1)$$

where the characteristic impedances of the transmission lines are normalized to 50 Ω and the frequency is normalized to the original center frequency $f_o = 1$ GHz. To simplify the calculation, the transmission lines have equal normalized characteristic impedances $\overline{Z_1} = \overline{Z_2} = \overline{Z_3} = \sqrt{2}$. $\theta_i \overline{f}$ (where i=1, 2, 3) represents the electrical length of each transmission line at normalized frequency $\overline{f}$. $\overline{Y} = 2\pi \overline{f} \cdot \overline{C_P}$ is the normalized admittance of the capacitor C_P. The normalized input impedance of port 1 at f_z should satisfy:

$$\overline{Z_{in}^{ev}} = \frac{\overline{A} + \overline{B}}{\overline{C} + \overline{D}} = 2 + j0 \quad (2)$$

The real part of the input impedance should satisfy $\mathrm{Re}(\overline{Z_{in}^{ev}}) = 2$. The capacitance C_P can be obtained by:

$$\overline{Y} = 2\pi \overline{f_z} \cdot \overline{C_P} = \frac{\tan(\theta_3 \overline{f_z})(\tan(\theta_1 \overline{f_z})\tan(\theta_2 \overline{f_z}) + 1)}{\sqrt{2}(\tan(\theta_1 \overline{f_z})\tan(\theta_3 \overline{f_z}) + \frac{2}{\cos(\theta_1 \overline{f_z})} - 2)} \quad (3)$$

where $\overline{f_z}$ is the normalized zero-reflection frequency. The imaginary part of the input impedance should satisfy $\mathrm{Im}(\overline{Z_{in}^{ev}}) = 0$. The relationship between θ_i (i=1, 2, 3) and $\overline{f_z}$ can be expressed as:

$$\frac{\frac{\tan(\theta_3 \overline{f_z})\tan(\theta_1 \overline{f_z}) + 1}{\tan(\theta_2 \overline{f_z})} - 2\tan(\theta_3 \overline{f_z}) - \tan(\theta_1 \overline{f_z})}{\frac{\tan(\theta_1 \overline{f_z})}{\tan(\theta_2 \overline{f_z})} - 2\tan(\theta_3 \overline{f_z})\tan(\theta_1 \overline{f_z}) + 4 - \frac{4}{\cos(\theta_1 \overline{f_z})}} = \frac{\tan(\theta_2 \overline{f_z})\tan(\theta_1 \overline{f_z}) + 1}{\frac{2}{\cos(\theta_1 \overline{f_z})} - 2 + \tan(\theta_1 \overline{f_z})} \quad (4)$$

To simplify the equation, some restrictive conditions could be assumed. For example, for Trantanella dividers, there is usually the condition of $\theta_2 = 90° - \theta_1$. For practical applications, the electrical length of the additional transmission lines θ_3 could be any value but is usually chosen between 0° to 15° referring to [3]. In this brief, θ_3 is 7°. For any chosen zero-reflection frequency $\overline{f_z}$ ($1 < \overline{f_z} < 3$), θ_1 can be obtained from (4), given that $\theta_2 = \pi/2 - \theta_1$ and θ_3 is a fixed value. Now the value of C_p can be calculated by (3). Some design examples are shown in Fig. 3. The original center frequency is

This article has been accepted for publication in a future issue of this journal, but has not been fully edited. Content may change prior to final publication. Citation information: DOI 10.1109/TCSII.2018.2803076, IEEE Transactions on Circuits and Systems II: Express Briefs

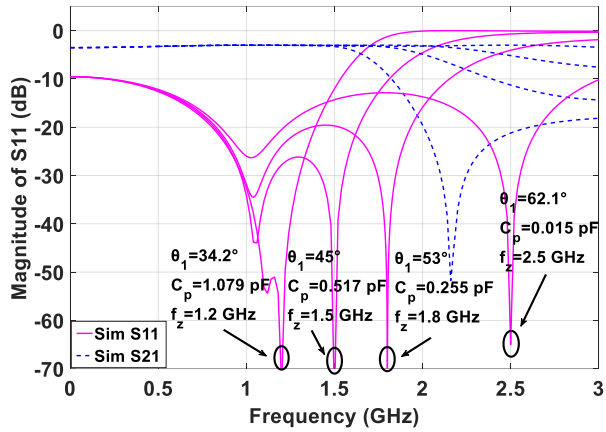

Fig. 3. Circuit parameters for realizing different additional zero-reflection frequencies.

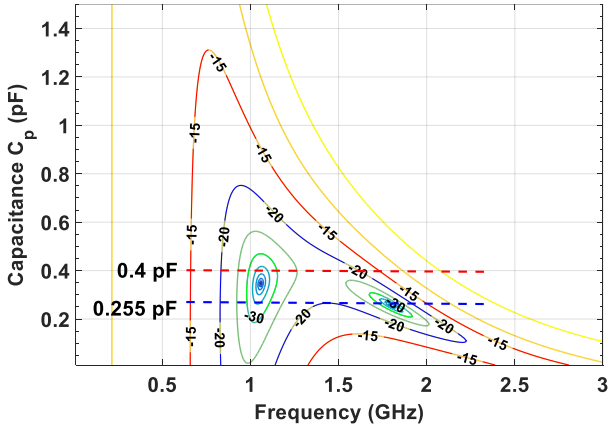

Fig. 4. The contours of S_{11} as a function of frequency and C_P when $\theta_1 = 53°$ and $\theta_3 = 7°$.

assumed to be 1 GHz and f_z is varied from 1.2 GHz to 2.5 GHz. By adding a pair of capacitors C_P, the reflection coefficient at the original center frequency is no longer zero (-∞ in dB), but the value is still very low (< -20 dB).

The minimum of the return loss S_{11} is changed slightly from the original center frequency, but still very close to 1 GHz ($1 < \bar{f} < 1.12$) according to (3), (4). Fig. 4 shows the contours of S_{11} as a function of the capacitance C_P with $\theta_1 = 53°$ and $\theta_3 = 7°$. The two dark areas represent the two low-reflection frequency zones at around 1.1 GHz and 1.8 GHz in this case. The -30 dB, -20 dB, and -15 dB contours are shown in the figure. When $\theta_1 = 53°$ and $\theta_3 = 7°$, the calculated C_P equals to 0.255 pF. For C_P = 0.255 pF, as shown in Fig. 4, S_{11} is slightly worse than -20 dB at around 1.4 GHz. If C_P is chosen to be 0.4 pF, S_{11} is better than -20 dB from $f_{L_{-20\,dB}} = 0.8$ GHz to $f_{H_{-20\,dB}} = 1.6$ GHz. Slightly decreasing C_P, the distance between $f_{L_{-20\,dB}}$ and $f_{H_{-20\,dB}}$ can be further extended. On the contrary,

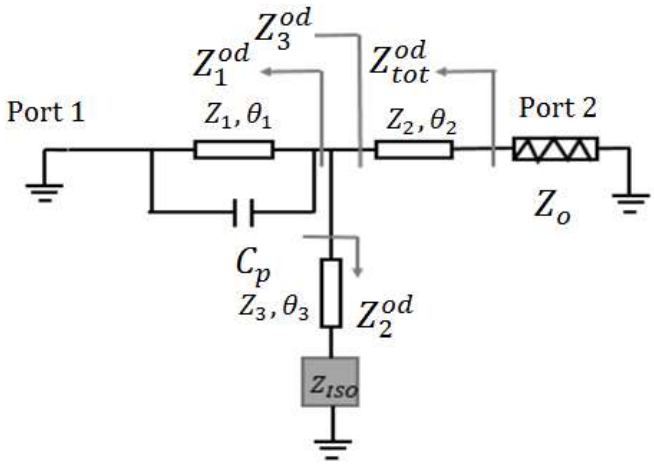

Fig. 5. Odd-mode equivalent circuit for the proposed divider.

the bandwidth will shrink when C_P increases. Therefore, the bandwidth of the proposed divider can be tuned in a wide range by fine tuning the capacitance C_P.

B. *Isolation Circuit*

The performance of isolation can be obtained by using the odd-mode analysis method. The theoretical values of components in the isolation circuit Z_{ISO} can be found under the condition of perfect matching for port 2 and port 3 at the center frequency $f_c = (f_0 + f_z)/2$. Fig. 5 shows the odd-mode equivalent circuit of the proposed power divider. $\overline{Z_1^{od}}$, $\overline{Z_2^{od}}$, $\overline{Z_3^{od}}$, and $\overline{Z_{tot}^{od}}$ are the normalized output impedances of the circuit respectively, and they can be obtained by using:

$$\overline{Z_1^{od}} = \frac{j\sqrt{2}\tan(\theta_1 \overline{f_c}) \cdot \frac{1}{j\overline{Y}}}{j\sqrt{2}\tan(\theta_1 \overline{f_c}) + \frac{1}{j\overline{Y}}} \tag{5}$$

$$\overline{Z_2^{od}} = \sqrt{2}\,\frac{\frac{\overline{Z_{ISO}}}{2} + j\sqrt{2}\tan(\theta_3 \overline{f_c})}{\sqrt{2} + j\frac{\overline{Z_{ISO}}}{2}\tan(\theta_3 \overline{f_c})} \tag{6}$$

$$\overline{Z_3^{od}} = \frac{\overline{Z_1^{od}} \cdot \overline{Z_2^{od}}}{\overline{Z_1^{od}} + \overline{Z_2^{od}}} \tag{7}$$

$$\overline{Z_{tot}^{od}} = \sqrt{2}\,\frac{\overline{Z_3^{od}} + j\sqrt{2}\tan(\theta_2 \overline{f_c})}{\sqrt{2} + j\overline{Z_3^{od}}\tan(\theta_2 \overline{f_c})} \tag{8}$$

$$\overline{Z_{ISO}} = -\frac{2\sqrt{2}(\tan(\theta_1 \overline{f_c}) + \tan(\theta_3 \overline{f_c}) - \tan(\theta_1 \overline{f_c})\tan(\theta_2 \overline{f_c})\tan(\theta_3 \overline{f_c}) - \sqrt{2}\overline{Y}\tan(\theta_1 \overline{f_c})\tan(\theta_3 \overline{f_c}))}{\sqrt{2}(\tan(\theta_1 \overline{f_c})\tan(\theta_2 \overline{f_c})\tan(\theta_3 \overline{f_c}) + \sqrt{2}\overline{Y}\tan(\theta_1 \overline{f_c})\tan(\theta_2 \overline{f_c}) - \tan(\theta_1 \overline{f_c}) - \tan(\theta_2 \overline{f_c})) + j[\tan(\theta_1 \overline{f_c})(\sqrt{2}\overline{Y} + \tan(\theta_2 \overline{f_c}) + \tan(\theta_3 \overline{f_c})) - 1]} \tag{9}$$
$$-\frac{2j(\sqrt{2}\overline{Y}\tan(\theta_1 \overline{f_c})\tan(\theta_2 \overline{f_c})\tan(\theta_3 \overline{f_c}) - \tan(\theta_1 \overline{f_c})\tan(\theta_2 \overline{f_c}) - \tan(\theta_2 \overline{f_c})\tan(\theta_3 \overline{f_c}) - \tan(\theta_1 \overline{f_c})\tan(\theta_3 \overline{f_c}))}{\sqrt{2}(\tan(\theta_1 \overline{f_c})\tan(\theta_2 \overline{f_c})\tan(\theta_3 \overline{f_c}) + \sqrt{2}\overline{Y}\tan(\theta_1 \overline{f_c})\tan(\theta_2 \overline{f_c}) - \tan(\theta_1 \overline{f_c}) - \tan(\theta_2 \overline{f_c})) + j[\tan(\theta_1 \overline{f_c})(\sqrt{2}\overline{Y} + \tan(\theta_2 \overline{f_c}) + \tan(\theta_3 \overline{f_c})) - 1]}$$

This article has been accepted for publication in a future issue of this journal, but has not been fully edited. Content may change prior to final publication. Citation information: DOI 10.1109/TCSII.2018.2803076, IEEE Transactions on Circuits and Systems II: Express Briefs

The output impedance $\overline{Z_{tot}^{od}}$ equals to 1 at the center frequency $\bar{f}_c$ for perfect matching at output ports. Thus, the total impedance in the isolation circuit can be derived by (9). The impedance Z_{ISO} can be calculated by instituting the design parameters of the transmission lines that described in the previous section. Since a series RLC is used in this design, we have:

$$\begin{cases} \mathrm{Re}\left(\overline{Z_{ISO}}\right) = \dfrac{\bar{R}}{2} \\ \mathrm{Im}\left(\overline{Z_{ISO}}\right) = 2\overline{\omega_C}\,\overline{L} - \dfrac{1}{2\overline{\omega_C}\,\overline{C}} \end{cases} \tag{10}$$

where $\overline{\omega_c}$ is the normalized center angle frequency. The relationship between design parameters (such as RLC) and perfect isolation performance among the circuit ports can be found through analyzing the network isolation using the method that was presented in [8]. The summation admittances of both circuit branches are zero when the circuit is perfectly isolated.

III. Experiment Results

A two-way power divider is designed and fabricated on a Rogers RT/5880 substrate with ε_r=2.2 as shown in Fig. 6(a). The thickness of the substrate is 0.79 mm and the conductor cladding is 35 μm thick. The circuit is measured by using a vector network analyser Agilent FieldFox N9917A.

The original center frequency is designed to be f_0 = 1 GHz and the ports terminations are 50 Ω. Firstly, $\theta_3 = 7°$and $Z_1 = Z_2 = Z_3 = 70.7\ \Omega$ are chosen. Then, to introduce an additional zero-reflection frequency f_Z at 1.8 GHz, the electrical length of the transmission lines and the capacitance C_P are calculated using (3) and (4) as $\theta_1 = 58°$ and C_P= 0.2 pF. The RLC on the isolation circuit can be calculated by using (9) and (10). RLC are further optimized by Sonnet software to maximize the S_{22} and S_{23} bandwidth. All the calculated and optimized design parameters are stated in Table I. The fabricated circuit has a compact size of 29 mm × 32 mm and the two output ports are widely apart.

The measured results of the proposed power divider with C_P=0.2 pF are shown in Fig. 7. It can be seen that a reflection zero is generated as expected and the operational bandwidth of the divider is significantly increased. As analyzed above, f_Z can be controlled by C_P. The measured results of the divider with $C_P = 0.4$ pF and $C_P = 0.8$ pF are also shown in Fig. 7. When $C_P = 0.8$ pF, there is only one reflection minimum located at around 1 GHz. Decreasing C_P to 0.4 pF, an additional reflection minimum appears in the upper passband which increases the bandwidth. Then further reducing C_P to 0.2 pF, the additional zero-reflection point is moved to around 1.9 GHz. In the measurement, the 15-dB-return-loss bandwidth starts from 0.7 GHz to 2.1 GHz. The fractional bandwidth achieves 100% ($f_{H-15\,dB}/\,f_{L-15\,dB} = 3{:}\,1$), which is much greater than that of traditional Wilkinson power dividers or typical Trantanella ones. In terms of reflection and isolation performance, S_{22} and S_{23} are also very good (<-15 dB) in the desired operational band as Fig. 7(b) shows. The measured insertion loss S_{21} is flat at around -3 dB over the whole operational band. Comparing the measurements in Fig. 7(a) (b) with the simulations in Fig. 8(a) (b), the measured results are in very good agreement with the simulations. Table II compares the measured performance of the two-way with other works. For two-way dividers, the useful bandwidth of the proposed one is much wider than others.

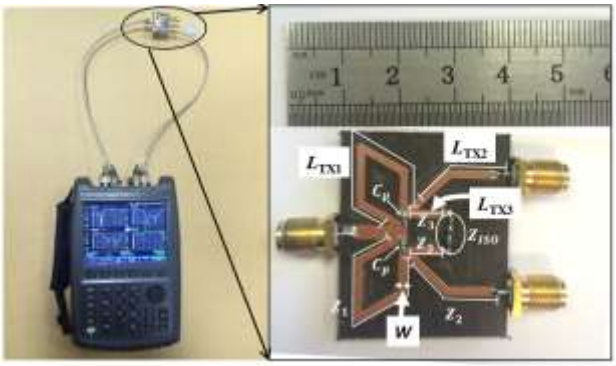

(a)

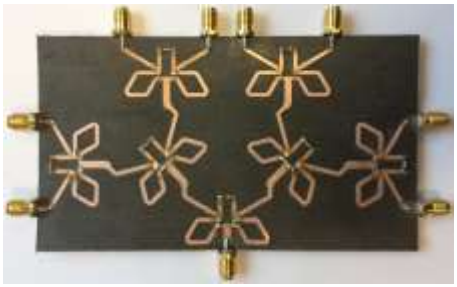

(b)

Fig. 6. Photographs of (a) the measurement set up and the fabricated two-way divider, and (b) the eight-way divider.

TABLE I
Comparison of Calculated and Optimized Parameters

Items	Cal.	Opt.	Items	Cal	Opt.
L_{TX1}	35.9 mm	38 mm	C_P	0.19 pF	0.2 pF
L_{TX2}	19.8 mm	22 mm	R	139Ω	130Ω
L_{TX3}	6.3 mm	8 mm	L	5 nH	3.9 nH
W	1.34 mm	1.35 mm	C	1.6 pF	1 pF

This method can also be applied to multi-way power divider designs. An eight-way three-section power divider is designed and fabricated for further demonstration as shown in Fig. 6(b). The parameters in each single section of the eight-way divider are almost identical to the two-way divider, which means no further changes on transmission lines need to be made for multi-way power dividers. The values of C_P and the lumped elements for the isolation circuits in different stages are optimized by simulation. The measured and simulated results for the eight-way power divider can be seen in Fig. 7(c) and Fig. 8(c), respectively. The S-parameters (scattering parameters) are better than -16 dB over the operating band in simulations. The measured return loss S_{11} and the output reflection S_{22} are better than -15 dB while the measured isolation S_{23} remains below

This article has been accepted for publication in a future issue of this journal, but has not been fully edited. Content may change prior to final publication. Citation information: DOI 10.1109/TCSII.2018.2803076, IEEE Transactions on Circuits and Systems II: Express Briefs

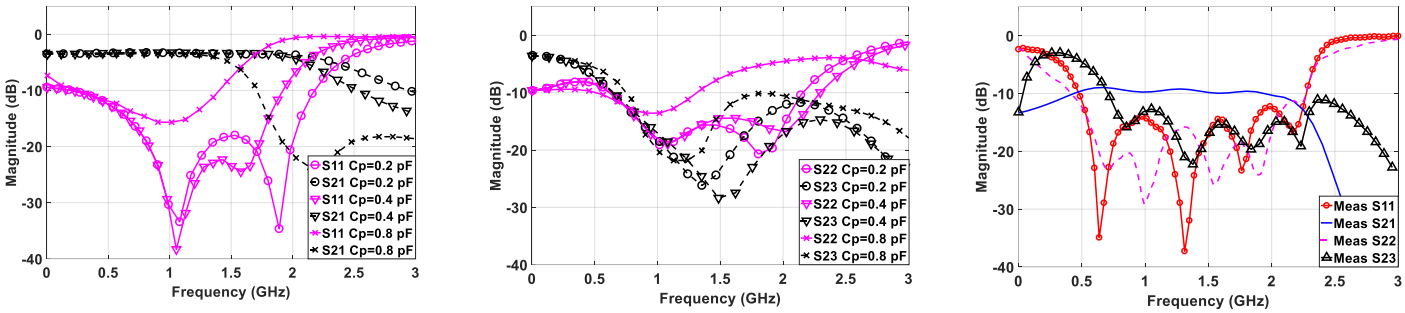

(a) (b) (c)

Fig. 7. Measured responses of (a) S_{11} & S_{21}, (b) S_{22} & S_{23} for different $\boldsymbol{C_P}$ of the two-way divider, (c) S_{11}, S_{21}, S_{22} and S_{23} for the eight-way power divider.

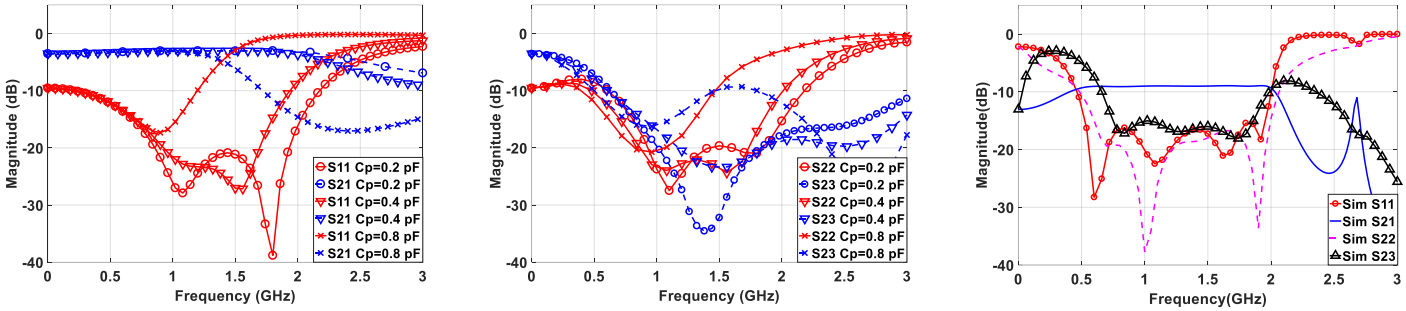

(a) (b) (c)

Fig. 8. Simulated results of (a) S_{11} & S_{21}, (b) S_{22} & S_{23} for different $\boldsymbol{C_P}$ of the two-way divider, (c) S_{11}, S_{21}, S_{22} and S_{23} for the eight-way power divider.

-13 dB. Comparing with the simulations, the offsets and deviation of S-parameters are probably caused by the fabrication error and the inaccuracy of the lumped elements. Overall, the measured results show good agreement with the simulated ones.

IV. Conclusions

Compact and wideband power dividers are more and more desirable in modern microwave communication systems. The Trantanella-type power dividers with the isolation circuit moved from the output ports to the middle of the transmission line can provide compact size and additional physical isolation. To broaden the operational bandwidth, a new design method has been proposed in this brief that a pair of capacitors can be added in parallel with the front-section transmission lines. The added capacitors have significantly increased the bandwidth of the power divider. The measured 15-dB-return-loss bandwidth of the two-way divider is 3:1 while the useful bandwidth in terms of other S-parameters is 2.73:1. For the eight-way divider, the measured 13-dB bandwidth is 2.67:1 considering all S-parameters while the return loss bandwidth can achieve 4.5:1. The simulated and measured results confirm that this proposed method can provide a broadband response compared to other works. In addition, changing the added capacitors will result in a wide tunable bandwidth (from 0 to 2.73: 1) of the dividers. Apart from the wide and tunable bandwidth, the proposed divider also has a compact size, and can provide physical separation as well as electrical isolation among output ports. Moreover, the measurement on the eight-way power divider has proved that this proposed method can be easily extended to multi-way divider designs.

TABLE II
Performance Comparison of Two-way Wilkinson-Type Power Dividers With Other Works

Reference	Circuit Size	Physical Isolation	Bandwidth (-15 dB)
[1]	$0.25\lambda_g$[1] *$0.02\lambda_g$	NO	2:1
[2]	$0.2\lambda_g$ *$0.05\lambda_g$	YES	NA
[3]	$0.25\lambda_g$*$0.06\lambda_g$	YES	1.45:1
[9]	$0.34\lambda_g$ *$0.2\lambda_g$	YES	1.85:1
This work	$0.12\lambda_g$ *$0.1\lambda_g$	YES	2.73:1

[1]: λ_g is the guided wavelength at the center frequency of the bandwidth.

References

[1] E. Wilkinson, "An N-way hybrid power divider," *IEEE Trans. Microw. Theory Thech.*, pp. 116-118, 19060.

[2] C-.J-.Trantanella, "A novel power divider with enhanced physical and electrical port isolation," *IEEE MTT-S Int.*, pp. 129-132, 2010.

[3] X. Wang, I. Sakagami, A. Mase, and M. Ichimura, "Trantanella Wilkinson power divider with additional transmission lines for simple layout.," *IET Microwaves, Antennas & Propagation*, vol. 8, no. 9, pp. 666-672, 2014.

[4] W.-J. Zhou and J.-X. Chen, "High-Selectivity Tunable Balanced Bandpass Filter With Constant Absolute Bandwidth," *IEEE Trans. Circuits Syst. II Exp. Briefs*, vol. 64, no. 8, pp. 917-921, 2017.

[5] W.-J. Feng, Y. Zhang and W.-Q. Che, "Tunable Dual-Band Filter and Diplexer Based on Folded Open Loop Ring Resonators," *IEEE Trans. Circuits Syst. II Exp. Briefs*, vol. 64, no. 9, pp. 1047-1051, 2017.

[6] T.Zhang and W.-Q. Che, "A compact Tunable Power Divider With Wide Tuning Frequency Range and Good Reconfigurable Resources," *IEEE Trans. Circuit Syst.II, Exp. Briefs*, vol. 63, no. 11, pp. 1054-1058, 2016.

[7] W.-D. Lin, R.-C. Liu, B.-L. Chen, P.-H. Deng and S.-F. Chao, "A Wilkinson power divider with transmission zero in desired stopband using embedded parallel resonator," in *Microwave Conference (APMC), 2014 Asia-Pacific*, Sendai, Japan , 2015.

[8] S.-Y. Hu, K. Song, and Y. Fan, "Planar ultra-wideband eight way power divider with improved isolation bandwidth," in *Microwave Confrence (APMC)*, Asia-Pacific. vol 2. IEEE, 2015.

[9] Mohammad A. M, Mohammad S. H and Fadhel M. G, "Theory and Design of a Novel Wideband DC Isolated," *Microwave and Wireless*, vol. 26, no. 8, pp. 586-588, 2016.